Chemical Engineering Science 276 (2023) 118820

Contents lists available at ScienceDirect

Chemical Engineering Science

journal homepage: www.elsevier.com/locate/ces

Short Communication

Scalable synthesis of highly exfoliated, water-dispersible boron nitride nanosheets for nano-fibrillated cellulose membrane toughening

Timo Elo [a], Vijay Singh Parihar [b], Riya Nag [c], Abhijit Bera [c], Rama Layek [a,*]

[a] LUT University, School of Engineering Science, Department of Separation Science, Mukkulankatu 19, 15210 Lahti, Finland
[b] Biomaterials and Tissue Engineering Group, BioMediTech, Faculty of Medicine and Health Technology, Tampere University, Finland
[c] Midnapore College (Autonomous), Raja Bazar Main Rd., 721101 Midnapore, India

ARTICLE INFO

Keywords:
Boron nitride nanosheet
Maleic anhydride
Diels Alder reaction
Nano-fibrillated cellulose
Membrane toughening

ABSTRACT

A very simple solid-state Diels Alder reaction of bulk boron nitride (BN) with maleic anhydride followed by ultrasonication in an aqueous solution was used to mass production of maleic acid functionalized highly exfoliated water dispersible single and few layers of boron nitride nanosheets (BNNS-MA). We demonstrate that as-synthesized BNNS-MA can be used to reinforce and toughen nano-fibrillated cellulose membranes.

1. Introduction

In recent years, the research on boron nitride nanosheets (BNNS) has attracted a great deal of attention due to its structural similarity with graphene and fascinating multi-functionalities (Wu et al., 2017). The BNNS has excellent physicochemical functionalities such as excellent mechanical properties, very good chemical and thermal stability, and outstanding thermal conductivity, as well as its unique electronic and optical properties compared to bulk BN sheets (Luo et al., 2017; Wu et al., 2017; Wu et al., 2022). Due to these outstanding functionalities, BNNS are currently considered as a very promising material for various demanding applications such as advanced polymer composites, barrier materials, optical sensors, thermal interface materials, UV-shielding materials and electro/analytical chemistry (Luo et al., 2017; Weng et al., 2016; Wu et al., 2017). One of the simplest routes to utilize these outstanding properties of BNNS is the uniform integration of BNNS into the polymer matrixes by utilizing interfacial interaction between BNNS and polymer matrixes (Weng et al., 2016). However, to harness these properties of the BNNS/polymer composites and bring them towards practical application and commercialization, a scalable production of highly exfoliated BNNS is extremely desirable.

There are primarily two strategies such as bottom-up (Luo et al., 2017; Steiner et al., 2019; Weng et al., 2016; Wu et al., 2017) and top-down (Luo et al., 2017; Tian et al., 2021; Weng et al., 2016; Wu et al., 2017) methods that have been explored to obtain exfoliated BNNS till now. In the bottom-up approaches such as chemical vapor deposition and arc discharge techniques, high quality of BNNS for electronic applications is produced from the mixture of boron and nitrogen sources (Luo et al., 2017; Steiner et al., 2019; Weng et al., 2016; Wu et al., 2017). Although the bottom-up methods can produce relatively high-quality BNNS, still, low yield, high cost of the precursors, costly instrument needed for production, critical synthetic condition (extremely high temperatures) and time-consuming processes have limited its mass production and commercialization. The top-down methods associated with the cutting of bulk BN sheets into nanosheets are more suitable for large-scale production of BNNS due to abundant and inexpensive raw materials and simple processes. The mechanical cleavage-based top-down method produces high-quality monolayer BNNS from bulk BN, however, the obtained quantity is very low (Luo et al., 2017; Tian et al., 2021; Weng et al., 2016; Wu et al., 2017). The BNNS produced by direct exfoliation of bulk BN via sonication (Chand et al., 2022) and ball milling (Wang et al., 2021) technique in liquid medium need drastic conditions that led to exfoliation of only a fraction of BN sheets into few layers. Hence, the use of BNNS is limited due to the lack of an effective method for the large-scale production of high-quality BNNS. To overcome this problem, very recently (Wang et al., 2023) an interesting method for the preparation of scalable quantity of BNNS via exfoliating pristine BN with liquid polyethyleneimine using a planetary ball mill machine where BNNS effectively exfoliated into monolayer nanosheets at high yields has been reported. To progress the synthesis and applications of BNNS research, there is a still a need for novel, and scalable BNNS synthesis route using a very simple preparation methodology.

* Corresponding author.
E-mail address: rama.layek@lut.fi (R. Layek).

https://doi.org/10.1016/j.ces.2023.118820
Received 8 February 2023; Received in revised form 14 April 2023; Accepted 26 April 2023
Available online 2 May 2023

Recently, several direct surface modifications of 2-D materials such as noncovalent functionalization, oxidation, cycloaddition, oxidation followed by cycloaddition, acylation and amidation of the hydroxyl groups, and the diazonium salts coupling have been developed to produce exfoliated 2-D sheets up (Layek and Nandi, 2013; Luo et al., 2017; Seo and Baek, 2014; Weng et al., 2016; Wu et al., 2017). Among them cycloaddition reaction is very promising, and both the recent simulation and experimental studies show the feasibility of Diels-Alder based cycloaddition to produce exfoliated 2-D nanosheets (Sarkar et al., 2011; Seo and Baek, 2014; Wang et al., 2020). Although there are few simulation and experimental studies for exfoliation of 2-D sheets, to the best of our knowledge there is no report of a simple approach for the scalable production of highly exfoliated and water dispersible BNNS via direct functionalization of BN powder through solid state Diels–Alder based cycloaddition reaction.

In this short communication, for the first time, we demonstrate a green and scalable production of highly exfoliated and water dispersible single and few layers of BNNS by simple Diels-Alder based cycloaddition reaction of bulk BN powder with maleic anhydride. Here BN powder acts as a diene and maleic anhydride acts as a dienophile and facilitates a thermal-assisted Diels-Alder based cycloaddition reaction. The BN powder functionalized maleic anhydride is converted into BN functionalized maleic acid (MA) in an aqueous solution and induces the delamination of the BN sheets with high efficiency to obtain scalable BNNS functionalized with MA (BNNS-MA) during the sonication in an aqueous solution. The application of the synthesized BNNS-MA in nanofibrillated cellulose (NFC) membrane toughening has been explored with a very low concentration of BNNS-MA integration. NFC is considered very promising for a wide variety of membrane such as polymer composite membranes for water purification, fuel cell membranes, packaging films, gas separation and gas barrier membranes due to its outstanding functionalities (Sharma et al., 2022; Shimizu et al., 2014; Widakdo et al., 2022). However, the NFC composite membranes are often less tough and brittle which limits their applications. To increase the toughness of NFC membranes, various techniques such as surface grafting (Layek et al., 2021) and blending with plasticizer-type molecules (Shimizu et al., 2014) have been reported; however, these methods reduce the mechanical strength of NFC membranes. It is reported that few NFC composite membranes do not enhance the strain of failure with nanofiller loading (Hu et al., 2022; Zhang et al., 2022). Despite the significant efforts in surface chemistries of nanoparticles and NFC film toughening, there is no report of NFC membrane toughening via judicially integrating a very low concentration of nanofiller. Here, we explored a very simple technique to produce a tough NFC membrane via judicially integrating as-synthesized BNNS-MA at low concentration.

2. Experimental

2.1. Materials

BN powder (1 μm, Sigma Aldrich, Germany) and maleic anhydride (VWR, Finland) and NFC (15 wt% solid content, University of Maine, USA) were used without any further purification.

2.2. Methods

2.2.1. Synthesis of BNNS-MA

The BNNS-MA was synthesized by direct functionalization of BN powder with maleic anhydride in an inert atmosphere at 180 °C followed by ultrasonication in an aqueous medium. Typically, the desired amount of BN powder (1 gm) was homogeneously mixed with maleic anhydride by mechanical grinding and then Diels–Alder reactions of this mixture were performed in a closed system under N_2 atmosphere at 180 °C for 4 h (Scheme 1). Then the obtained product was transferred to an aqueous medium and sonicated for 30 min. During sonication, the BN layers easily exfoliated and dispersed into an aqueous solution. Then, the solution was filtrated through a nylon membrane and washed with milli-Q water for several times to remove unreacted reagent and finally dried in a vacuum oven at 50 °C for 24 h to obtain BNNS-MA.

2.2.2. Preparation of BNNS-MA / NFC composite

Then, BNNS-MA/NFC composite membranes were produced using a vacuum-assisted assembly technique (ESI Fig. 1). At first, aqueous dispersions of BNNS-MA and NFC were prepared by ultra-sonication for 2 min and 30 min separately. Typically, the homogeneous BNNS-MA/NFC solution was produced by combining a desired amount of aqueous dispersions of BNNS-MA with a desired amount of aqueous dispersion of NFC (1 mg/mL), followed by sonication for 5 min. The BNNS-MA/NFC aqueous dispersion was then vacuum filtered and dried at room temperature overnight before being pressed at 70 °C for 5 min. 0.5 wt% and 1 wt% BNNS-MA integrated NFC composite membranes were prepared and designated as BNNS-MA 0.5 and BNNS-MA 1 respectively. Pure NFC membrane was prepared in the same way but without the addition of BNNS-MA.

2.2.3. Characterization

The zeta potential and high-resolution transmission electron microscopy (HRTEM) studies of the aqueous dispersion of BNNS-MA were performed by laser granulometry (Zetasizer Nano ZS, Malvern, UK) and Jeol F200 S/TEM instrument respectively. The atomic force microscopy (AFM) and scanning tunneling microscopy (STM) studies of the BNNS-MA were performed by using an XE-7, Park AFM (Park Systems Corp., South Korea) with a Pt-Ir tip of 0.25 mm diameter and a 20 nm tip-apex

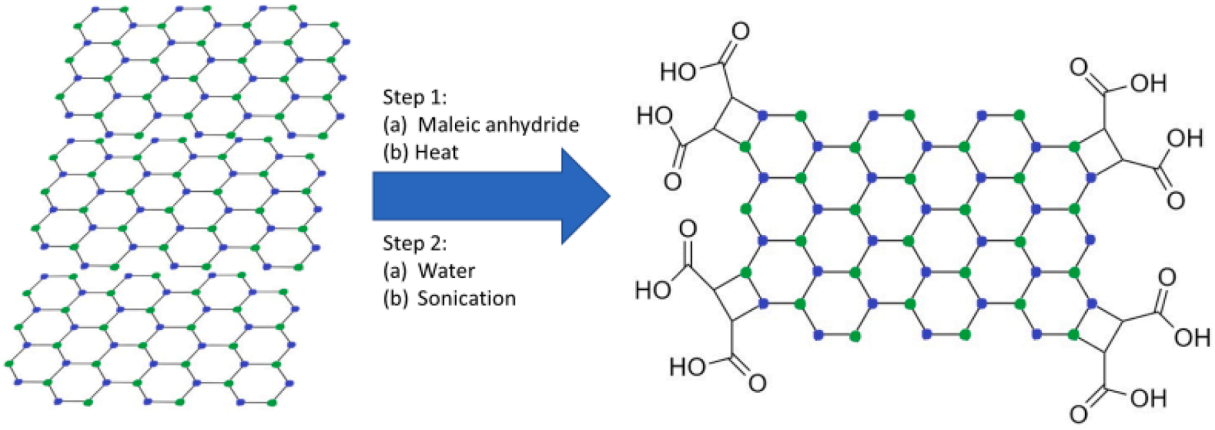

Scheme 1. Scheme for the preparation of BNNS-MA.

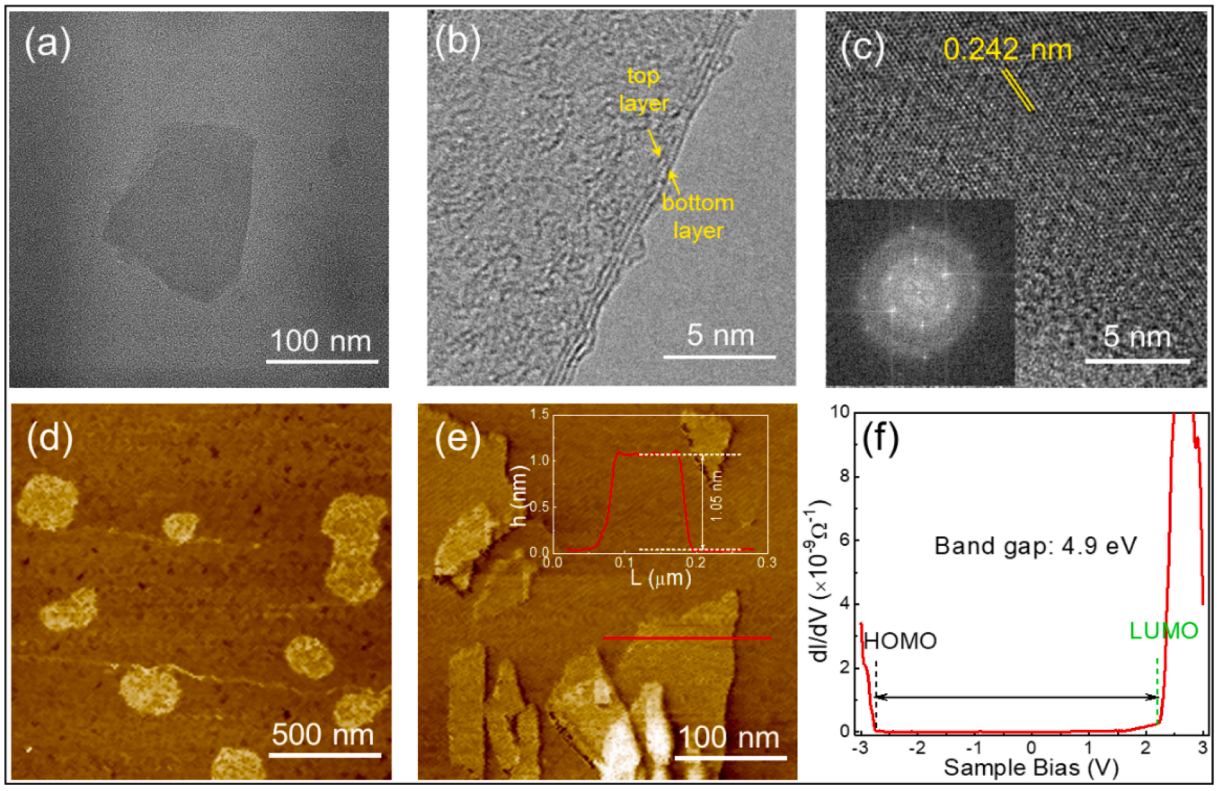

Fig 1. HRTEM, AFM, STM and corresponding height profile and density of states spectra of hBNNS layer.

(approx.) at a scan rate of 0.5 Hz. TGA and Raman spectra studies of BN and BNNS-MA were performed by TGA-Q-500 instrument in a nitrogen atmosphere at a heating rate of 10 °C/min and Renishaw InVia Qontor spectrometer with a laser excitation wavelength of 532 nm respectively. Wide angle x-ray scattering spectroscopy (WAXS) of BN and BNNS-MA was carried out using a Bruker AXS D8 ADVANCE instrument. Field emission electron microscopy (FESEM) study of the cryo-fractured NFC composite membrane was performed by JEOL JSM-7900F instrument after sputtering platinum. A Bruker Alpha-P instrument was used to record the FTIR spectra of NFC and BNNS-MA/NFC composite membranes in ATR mode with a diamond tip in the 4000–400 cm^{-1} range. Mechanical testing of the NFC composite membrane was performed using Instron 5967 instrument.

3. Result and discussion

3.1. Functionalization and exfoliation BNNS:

Bulk BN powder consists of many layers of BN sheets with a distance between layers ~0.33 nm. Each layer consists of conjugated aromatic rings and therefore strong VDW interaction is present between the layers. It is hydrophobic and remains a multi-layered agglomerated material in an aqueous medium. With sonication, BN sheets produce a white color aqueous dispersion (1 mg/mL) with very poor dispersion stability. Most of these BN sheets are precipitated from the aqueous solution within 5 min which indicates that no satisfactory exfoliation of BN occurs to produce a high quantity of BNNS. But when BNNS-MA was sonicated for 5 min (1 mg/mL), a white color aqueous dispersion with a negative zeta potential value of −27 mV is produced and no precipitation occurs from the solution. This indicates that a large quantity of BNNS-MA is highly exfoliated in an aqueous medium and produces a very stable homogeneous dispersion. The unsaturated unit of MA is covalently linked by cycloaddition reaction with BNNS like other 2-D materials (Sarkar et al., 2011; Seo and Baek, 2014; Wang et al., 2020), and there are two –COOH groups per MA unit in BNNS-MA. The cyclic ring produced by the cycloaddition reaction can interact with the aromatic sheet structure of BN by covalent interactions which can decrease the VDW interaction among the layers of BN. The –COOH groups of MA have a strong affinity toward the polar solvent like water. Hence it can help to decrease the VDW interaction among the layers of BN in an aqueous medium which causes large-scale exfoliation of BN via ultrasonication.

The morphology, nature of exfoliation and presence of several layers were investigated by casting a drop of a dilute aqueous dispersion of BNNS-MA on the desired substrate and examining them utilizing HRTEM, AFM and STM and the images are presented in Fig. 1 ((a)-(f)). The TEM image of BNNS-MA indicates that in a dilute aqueous medium, it remains as highly exfoliated sheets ((Fig. 1(a)-(c)). The HRTEM image of the edge of BNNS-MA shows a few lines on the edge of BNNS-MA (Fig. 1(b)), which confirms the existence of a few layers of BNNS-MA sheets in a dilute aqueous solution (Yu et al., 2015). Both the AFM and STM images of BNNS-MA (Fig. 1 (d) & (e)) display a structure that resembles sheets. The apparent height of most BNNS-MA sheets is approximately 0.67–1.05 nm, according to the height profile analysis of the STM image. The interlayer distance between the bulk BN is ≈ 0.33 nm. The results of the height profile analysis from the STM study by casting a drop from an aqueous solution of BNNS-MA indicate the presence of a few layers of highly exfoliated BNNS in an aqueous medium. The measured electronic band gap of the BNNS-MA sheet from the density of states spectra (Fig. 1 (f)) is 4.9 eV matched well with the monolayer BNNS sheet. (Ekuma et al., 2017). In the literature it is found that the lateral size of the boron nitride nanosheets depend on the size of starting BN material and methods used for the preparation of boron nitride nanosheets, whereas numbers of layers depend on the method used for the BNNS synthesis (Chand et al., 2022; Chen et al., 2019; Fan et al., 2016; Han et al., 2021; Ji et al., 2020; Lei et al., 2015; Li et al., 2011; Tian et al., 2021; Wang et al., 2021; Wang et al.,2023). In our study, we observed that majority of BNNS-MA show 2–3 sheets along with few single sheets. A comparison of the lateral size and number of layers obtained by our method and other mechanical exfoliation

methods reported in literature are presented in ESI Table S1.

Thermogravimetry analysis (TGA) of BN and BNNS-MA (Fig. 2(a)) was carried out to get an idea about the thermal stability and the degree of MA functionalization in BNSS-MA. From the figure, it is clear that BN does not show any weight loss in the temperature range of 50–550 °C. There is approximately no, or negligible weight loss shown by BNNS-MA in the temperature range below 100 °C which indicates that there is no absorbed water molecule present in the BNNS after drying in a vacuum at 50 °C. After that, 150–450 °C BNNS shows a gradual weight loss compared to bulk BN powder. The higher degradation of BNNS in the temperature range of 150–450 °C compared to bulk BN is due to the decomposition of the MA unit of BNNS-MA. The total weight for MA unit degradation is ~1 wt%, and it indicates the ~1 wt% of MA has been functionalization in BNNS-MA. In Diels-Alder reaction the BN is used as 4 π diene system and maleic anhydride as 2 π dienophile. It is reported both theoretically and experimentally that the Diels-Alder reaction of 2-D materials occurs only through the edges of the 2-D sheets and the basal plane does not take part in the reaction (Seo and Baek, 2014; Wang et al., 2020). Hence, there are a limited number of reaction sites available in 2-D BN for the Diels-Alder reaction which causes a lower degree of MA functionalization of 1 wt% in BNNS-MA. Wide angle x-ray scattering (WAXS) of BN and BNNS-MA (ESI Fig. 2) was carried out to investigate the structure and exfoliation in the solid state from the relative intensity of the peak. Pristine BN powder shows a highly intense characteristic diffraction peak at $2\theta = 27^{\circ}$ which represents 002 plane and indicates the distance between the layer ~ 0.33 nm (Harrison et al., 2019; Liu et al., 2019). In BNNS-MA, there is no shift of the peak position of the 002 plane with respect to BN and it indicates that the interplanar distance of the BNNS-MA remains the same as bulk BN powder. As the MA molecules are functionalized at the edges of BN to produce BNNS-MA, and hence the MA molecules remain at the edge of BNNS-MA, not at the basal plane of BNNS-MA. Therefore, in a solid state, the distance between the sheets of BNNS-MA remains the same as BN powder. However, the peak intensity of the BNNS-MA is significantly decreased compared to bulk BN powder. The decrease in intensity of the WAXS peak compared to BN powder indicates the existence of a few layers of sheets in BNNS-MA in the solid state. However, BNNS-MA produces a highly exfoliated sheet with single and few layers in an aqueous solution as proved by HRTEM, AFM and STM results. Furthermore, to investigate the electronic structure and nature of exfoliation of BNNS-MA, the Raman spectroscopy study of BN and BNNS-MA were performed and illustrated in Fig. 2 (b). One can understand from the figure that pristine BN powder shows only one Raman peak with high intensity at ≈1365.28 cm^{-1} which is analogous to the G band of graphene and can be attributed to the in-plain E2g mode vibration of BN (Xiao et al., 2015; Harrison et al., 2019; Nag et al., 2022). It is reported that the Raman peak intensity progressively decreases, and the peak position is red shifted with increasing degree of exfoliation and decreasing number of layers of BN under the same measurement conditions. From the figure, it is obvious that the intensity of this G band of BNNS-MA becomes significantly weaker and redshifted from 1365.28 cm^{-1} to 1363.89 cm^{-1} with respect to bulk BN powder. Hence, it indicates that the BNNS-MA exhibits a highly exfoliated structure, and most of the sheets are exfoliated into few layers of nanosheets.

3.2. NFC composite membrane with BNNS-MA

Scalable production and a high degree of exfoliation in aqueous solution opens new application possibilities for this novel as-synthesized BNNS-MA, for example for improving the mechanical strength and toughness of NFC-based composite membranes. NFC is an amphiphilic biopolymer and hence, sonication of it in an aqueous medium produces a stable aqueous suspension. Sonication of a colloidal BNNS-MA dispersion with an aqueous suspension of NFC, produced a homogeneous BNNS-MA/NFC aqueous suspensions and vacuum filtration produced free-standing BNNS-MA/NFC composite films by removing water from these aqueous suspensions (ESI Fig. 1). 0.5 and 1 wt% of BNNS-MA integrated NFC composite films were fabricated. The composite film formation was governed by physical interaction between the functional moiety of BNNS-MA and amphiphilic NFC, as well as judicial nano integration.

To investigate the cross-sectional morphology and structure of the composite film, the FESEM images of cryo-fractured cross-sections of NFC and BNNS-MA/NFC composites membranes are presented in ESI Fig. 3 and Fig. 3 (a)-(b). The AFM image and the corresponding height profile of pure NFC that was performed via casting a drop of dilute aqueous solution shows a diameter of less than 10 nm of the fibres (ESI Fig. S4) and it indicates that NFC remains individually dispersed in dilute aqueous solution. During the vacuum filtration process, these individually dispersed NFC fibrils are stacked together to produce an assembled fibre structure. This phenomenon is evident from the cross-sectional FESEM images. From ESI Fig. 3 and Fig. 3 (a) & (b), it is obvious that NFC fibrils produce a morphology of the assembled NFC fibres both in the NFC and BNNS-MA/NFC composite membranes and it indicates that integration of low concentration of BNNS-MA does not alter the fibrillar structure of NFC membrane significantly. The FESEM image of pure NFC membrane has a homogeneous stacked fibrillar structure, whereas in the composite films the exfoliated BNNS-MA

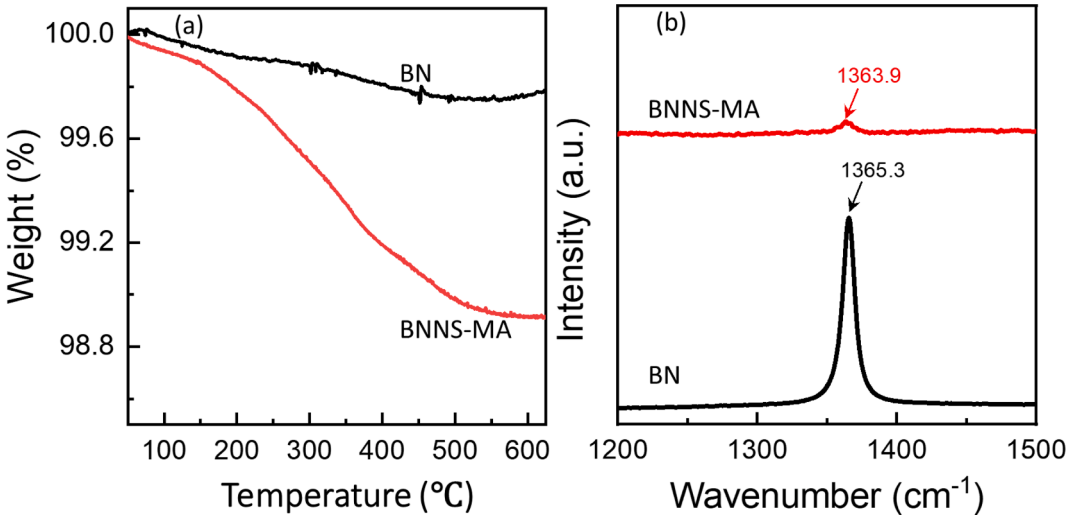

Fig. 2. (a) TGA and (b) Raman spectra of BN and BNNS-MA.

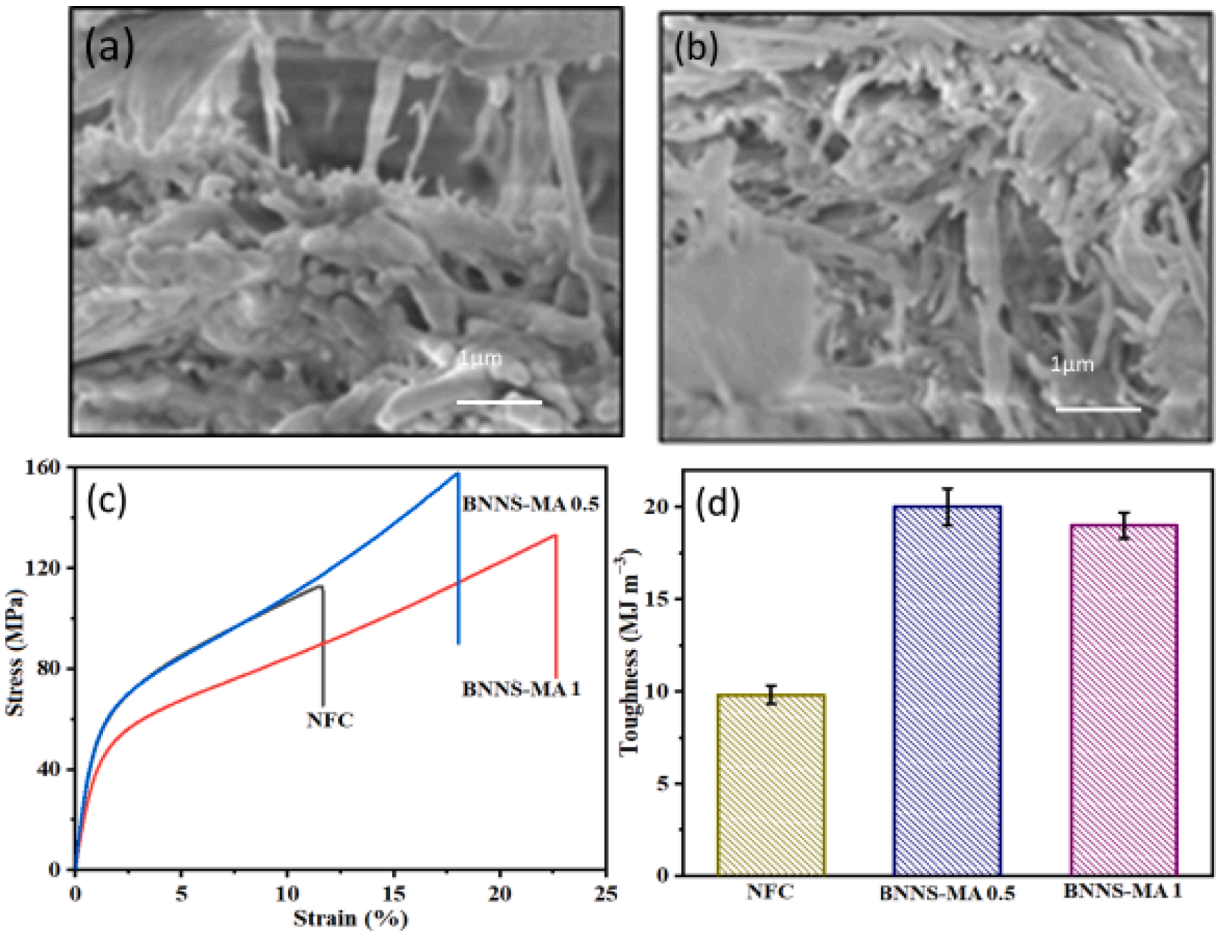

Fig 3. FESEM images ((a) = BNNS-MA 0.5; (b) = BNNS-MA 1) and mechanical properties (c,d) of the BNNS-MA/NFC composites.

sheets are well dispersed throughout the assembled NFC matrix which has a significant influence on the mechanical behavior of the NFC membrane.

To examine the mechanical behavior of the BNNS-MA/NFC composite membrane, the stress–strain curves of the NFC and BNNS-MA/NFC composite membranes are shown in Fig. 3 (c) in tensile mode. The pure NFC film has a tensile strength of 107 ± 5 MPa and an elongation at a break of 11.5 ± 2% with a toughness value of 9.20 MJ m^{-3}. Due to the high aspect ratio and interfacial interaction between 2-D BNNS-MA and NFC, we anticipated that BNNS-MA integration at low concentration in NFC membrane could enhance mechanical strength with a significant decrease of strain at the failure to form a brittle composite membrane like other polymers composite system (Hu et al., 2022). However, we revealed that when very small amounts of BNNS-MA (0.5 wt% and 1 wt%) were integrated, the elongation at break increased significantly with simultaneous enhancement stress at break compared to pure NFC membrane. Only with 0.5 wt% BNNS-MA loading, the NFC composite membrane exhibits a clear improvement of tensile strength from 107 ± 5 MPa to 135 ± 3 MPa with an increase in strain % at break from 11.5 ± 2 % to 23 ± 1.5% (ESI Fig. S5 (a)& (b)). To explain this type of mechanical behavior, we proposed an interaction between NFC and BNNS-MA that comprises a reduction of H-bonding interaction between the –OH group of NFC, introduction of interfacial interaction between –COOH group of BNNS-MA and –OH group of NFC, CH-π-interactions between hydrophobic cellulosic backbone of NFC chain with π cloud of BNNS-MA. It is reported in theoretical study that CH groups of glucopyranose of cellulose chains interact with a π cloud of aromatic rings of graphene via CH-π interaction (Alqus et al., 2015). Since BNNS-MA has aromatic rings that are analogous to that of graphene, there is a possibility of BNNS-MA to interact with NFC via CH-π interaction in a similar fashion of graphene integrated cellulose composites. The shifting of the C–H stretching vibration peak position of the CH group of polymer chain in FTIR spectra serves as evidence for the CH-π interaction between the π cloud of carbon nanotubes and the CH groups of the polymer chain according to earlier report (Garai et al., 2009). Therefore, the FTIR spectra of the NFC and BNNS-MA/NFC composite membranes were shown in ESI Fig. S6 to illustrate the interfacial interaction between NFC and BNNS-MA. It is clear from the FTIR spectra of pure NFC that the stretching vibrations of the H-bonded –OH groups and the C–H stretching vibrations of the CH groups of the glucopyranose unit of NFC exhibit a typical broad peak at 3311 cm^{-1} and sharp peaks at 2916 /2850 cm^{-1} respectively. The BNNS-MA/NFC composite membranes exhibit all the peaks of NFC. However, C–H stretching vibration band is slightly shifted from 2916 cm^{-1} to 2920 cm^{-1} in the BNNS-MA/NFC composite membranes and this might be due to the CH–π interaction between CH groups of glucopyranose of NFC and π cloud of BNNS-MA (Garai et al., 2009). In addition, the –OH stretching vibration peak becomes broader and slightly shifted from 3311 cm^{-1} to 3307.5 cm^{-1} in the BNNS-MA 0.5 and this might be due to blocking of H-bonding sites of NFC by BNNS-MA. This type of combined interaction has not been proposed previously, however, we are proposing the existence of such types of interactions as it can correlate to mechanical testing results of BNNS-MA/NFC composite membrane. The integration of highly dispersed BNNS-MA without aggregation at low concentration in NFC membrane can block the H-bonding sites of adjacent cellulose nanofibril through the basal plane of the 2-D structure. It can reduce the H-bonding interaction between adjacent NFC fibrils and introduce a plasticizing/lubricating property in the NFC

composite membrane that led to higher strain% at failure compared to pure NFC membrane. The –COOH group of BNNS-MA at the edge can interact with the –OH group of NFC through H-bonding, and the π cloud of BNNS-MA can interact with the C–H moiety of the hydrophobic cellulosic backbone of the NFC chain that can cause enhancement of stress at the break via interfacial load transfer from NFC to BNNS-MA similar to other polymers nanocomposite system (Hu et al., 2022; Malho et al., 2012). The combination of increased tensile stress and strain at failure in BNNS-MA/NFC composite membranes resulted in significant toughness improvement compared to NFC membrane. Only 0.5 wt% BNNS-MA integrated NFC composite membrane produces a significant increase in toughness from 9.2 MJ m^{-3} to 20 MJ m^{-3} (Fig. 3 (d)), indicating a synergetic composite property of superior toughness compared to pure NFC membrane through tailoring stress at break and strain % at failure.

4. Conclusion

In summary, we have established a very simple and extremely effective procedure to prepare a highly exfoliated single and few layers of BNNS in mass scale from bulk BN powder for the first time through Diels-Alder reaction that sidesteps the drastic reaction conditions/or hazardous oxidation reactions of bulk BN. The Diels-Alder reaction assisted the covalent functionalization of BN powder with MA and ultrasonic wave treatment in an aqueous medium to govern the delamination and exfoliation as well as the scalable formation of BNNS-MA. The obtained BNNS-MA exhibited excellent dispersion in an aqueous medium and was used to fabricate a composite membrane with NFC with higher toughness from an aqueous dispersion of BNNS-MA/NFC composite using a vacuum filtration method. The NFC composite membranes at a very low concentration of BNNS-MA content of 0.5 wt% shows observable higher strength, flexibility and toughness compared to pure NFC membrane. Overall, our research demonstrated a scalable synthesis of highly exfoliated BNNS-MA and its reinforcement in NFC membranes that opens new avenues for the processing of innovative biopolymer composite membranes with tailored functionalities.

Declaration of Competing Interest

The authors declare that they have no known competing financial interests or personal relationships that could have appeared to influence the work reported in this paper.

Data availability

Data will be made available on request.

Acknowledgements

This study was supported by Kollin säätiö funding for biorefinery research at LUT University, Lahti campus. AB acknowledge SERB, India grant under file no. EEQ/2020/000156.

Appendix A. Supplementary data

Supplementary data to this article can be found online at https://doi.org/10.1016/j.ces.2023.118820.

References

Alqus, R., Eichhorn, S.J., Bryce, R.A., 2015. Molecular Dynamics of Cellulose Amphiphilicity at the Graphene-Water Interface. Biomacromolecules; Biomacromolecules 16 (6), 1771–1783.

Chand, H., Kumar, A., Bhumla, P., Naik, B. R., Balakrishnan, V., Bhattacharya, S., Krishnan, V., 2022. Scalable Production of Ultrathin Boron Nanosheets from a Low-Cost Precursor, Advanced materials interfaces 9(23), 2200508-n/a.

Chen, S., Xu, R., Liu, J., Zou, X., Qiu, L., Kang, F., Liu, B., Cheng, H., 2019. Simultaneous Production and Functionalization of Boron Nitride Nanosheets by Sugar-Assisted Mechanochemical Exfoliation, Advanced materials (Weinheim); Adv Mater 31(10), e1804810-n/a.

Ekuma, C.E., Dobrosavljević, V., Gunlycke, D., 2017. First-Principles-Based Method for Electron Localization: Application to Monolayer Hexagonal Boron Nitride, Physical Review Letters. Phys Rev Lett 118 (10), 106404.

Fan, D., Feng, J., Liu, J., Gao, T., Ye, Z., Chen, M., Lv, X., 2016. Hexagonal boron nitride nanosheets exfoliated by sodium hypochlorite ball mill and their potential application in catalysis. Ceramics International 42 (6), 7155–7163.

Garai, A., Kuila, B.K., Samai, S., Roy, S., Mukherjee, P., Nandi, A.K., 2009. Physical and electronic properties in multiwalled carbon nanotube–poly(3-dodecylthiophene) nanocomposites. Journal of polymer science.Part B, Polymer physics 47 (14), 1412–1425.

Han, G., Zhao, X., Feng, Y., Ma, J., Zhou, K., Shi, Y., Liu, C., Xie, X., 2021. Highly flame-retardant epoxy-based thermal conductive composites with functionalized boron nitride nanosheets exfoliated by one-step ball milling. Chemical Engineering Journal 407, 127099.

Harrison, H., Lamb, J.T., Nowlin, K.S., Guenthner, A.J., Ghiassi, K.B., Kelkar, A.D., Alston, J.R., 2019. Quantification of hexagonal boron nitride impurities in boron nitride nanotubes via FTIR spectroscopy. Nanoscale advances 1 (5), 1693–1701.

Hu, D., Liu, H., Guo, Y., Yang, M., Ma, W., 2022. Interfacial design of nanocellulose/boron nitride nanosheets composites via calcium ion cross-linking for enhanced thermal conductivity and mechanical robustness, Composites. Part A, Applied science and manufacturing 158, 106970.

Ji, D., Wang, Z., Zhu, Y., Yu, H., 2020. One-step environmentally friendly exfoliation and functionalization of hexagonal boron nitride by β-cyclodextrin-assisted ball milling. Ceramics International 46 (13), 21084–21089.

Layek, R.K., Nandi, A.K., 2013. A review on synthesis and properties of polymer functionalized graphene. Polymer (Guilford) 54 (19), 5087–5103.

Layek, R.K., Parihar, V.S., Seppälä, J., Efimov, A., Palola, S., Kanerva, M., Annurakshita, S., Kellomäki, M., Sarlin, E., 2021. Reduced graphene oxide integrated poly(ionic liquid) functionalized nano-fibrillated cellulose composite paper with improved toughness, ductility and hydrophobicity. Materials advances 2 (3), 948–952.

Lei, W., Mochalin, V.N., Liu, D., Qin, S., Gogotsi, Y., Chen, Y., 2015. Boron nitride colloidal solutions, ultralight aerogels and freestanding membranes through one-step exfoliation and functionalization, Nature communications. Nat Commun 6 (1), 8849.

Li, L.H., Chen, Y., Behan, G., Zhang, H., Petravic, M., Glushenkov, A.M., 2011. Large-scale mechanical peeling of boron nitride nanosheets by low-energy ball milling. Journal of materials chemistry 21 (32), 11862–11866.

Liu, Q., Hu, C., Wang, X., 2019. One-pot solvothermal synthesis of water-soluble boron nitride nanosheets and fluorescent boron nitride quantum dots. Materials letters 234, 306–310.

Luo, W., Wang, Y., Hitz, E., Lin, Y., Yang, B., Hu, L., 2017. Solution Processed Boron Nitride Nanosheets: Synthesis, Assemblies and Emerging Applications, Advanced functional materials 27(31), 1701450-n/a.

Malho, J., Laaksonen, P., Walther, A., Ikkala, O., Linder, M.B., 2012. Facile Method for Stiff, Tough, and Strong Nanocomposites by Direct Exfoliation of Multilayered Graphene into Native Nanocellulose Matrix. Biomacromolecules 13 (4), 1093–1099.

Nag, R., Layek, R.K., Bera, A., 2022. Functionalized MXene Nanosheets and Al-Doped ZnO Nanoparticles for Flexible Transparent Electrodes. ACS applied nano materials 5 (12), 17939–17948.

Sarkar, S., Bekyarova, E., Niyogi, S., Haddon, R.C., 2011. Diels−Alder Chemistry of Graphite and Graphene: Graphene as Diene and Dienophile, Journal of the American Chemical Society. J. Am. Chem. Soc 133 (10), 3324–3327.

Seo, J., Baek, J., 2014. A solvent-free Diels-Alder reaction of graphite into functionalized graphene nanosheets, Chemical communications (Cambridge, England). Chem Commun (Camb) 50 (93), 14651–14653.

Sharma, S.K., Sharma, P.R., Wang, L., Pagel, M., Borges, W., Johnson, K.I., Raut, A., Gu, K., Bae, C., Rafailovich, M., Hsiao, B.S., 2022. Nitro-oxidized carboxylated cellulose nanofiber based nanopapers and their PEM fuel cell performance. Sustainable energy & fuels 6 (15), 3669–13368.

Shimizu, M., Saito, T., Fukuzumi, H., Isogai, A., 2014. Hydrophobic, Ductile, and Transparent Nanocellulose Films with Quaternary Alkylammonium Carboxylates on Nanofibril Surfaces. Biomacromolecules; Biomacromolecules 15 (11), 4320–4325.

Steiner, D., Mittendorfer, F., Bertel, E., 2019. Quasiliquid Layer Promotes Hexagonal Boron Nitride (h-BN) Single-Domain Growth: h–BN on Pt(110), ACS nano. ACS Nano 13 (6), 7083–7090.

Tian, X., Wu, N.i., Zhang, B., Wang, Y., Geng, Z., Li, Y., 2021. Glycine functionalized boron nitride nanosheets with improved dispersibility and enhanced interaction with matrix for thermal composites. Chemical Engineering Journal 408, 127360.

Wang, W., Wang, C., Zheng, J., Shang, F., Dang, J., Zhao, X., 2020. Directional Diels-Alder cycloadditions of isoelectronic graphene and hexagonal boron nitride in oriented external electric fields: reaction axis rule vs. polarization axis rule. Nanoscale 12 (28), 15364–15370.

Wang, Z., Wei, X., Bai, M., Lei, J., Xu, L., Huang, H., Du, J., Dai, K., Xu, J., Li, Z., 2021. Green Production of Covalently Functionalized Boron Nitride Nanosheets via Saccharide-Assisted Mechanochemical Exfoliation, ACS sustainable chemistry & engineering. ACS Sustainable Chem. Eng 9 (33), 11155–11162.

Wang, Z., Yan, X., Hou, Q., Liu, Y., Zeng, X., Kang, Y., Zhao, W., Li, X., Yuan, S., Qiu, R., Uddin, M.H., Wang, R., Xia, Y., Jian, M., Kang, Y., Gao, L., Liang, S., Liu, J.Z., Wang, H., Zhang, X., 2023. Scalable high yield exfoliation for monolayer nanosheets, Nature communications. Nat Commun 14 (1), 236.

Weng, Q., Wang, X., Wang, X., Bando, Y., Golberg, D., 2016. Functionalized hexagonal boron nitride nanomaterials: emerging properties and applications, Chemical Society Reviews. Chem Soc Rev 45 (14), 3989–13412.
Widakdo, J., Austria, H.F.M., Subrahmanya, T.M., Suharyadi, E., Hung, W., Wang, C., Hu, C., Lee, K., Lai, J., 2022. Switching gas permeation through smart membranes by external stimuli: a review. Journal of materials chemistry.A, Materials for energy and sustainability 1 (32), 16743–111676.
Wu, M., Zhou, Y., Zhang, H., Liao, W., 2022. 2D Boron Nitride Nanosheets for Smart Thermal Management and Advanced Dielectrics, Advanced materials interfaces 9 (25), 2200610-n/a.
Wu, K., Fang, J., Ma, J., Huang, R., Chai, S., Chen, F., Fu, Q., 2017. Achieving a Collapsible, Strong, and Highly Thermally Conductive Film Based on Oriented Functionalized Boron Nitride Nanosheets and Cellulose Nanofiber. ACS applied materials & interfaces 9 (35), 30035–30045.
Xiao, F., Naficy, S., Casillas, G., Khan, M.H., Katkus, T., Jiang, L., Liu, H., Li, H., Huang, Z., 2015. Edge-Hydroxylated Boron Nitride Nanosheets as an Effective Additive to Improve the Thermal Response of Hydrogels. Advanced materials (Weinheim) 27 (44), 7196–7203.
Yu, J., Li, J., Zhang, W., Chang, H., 2015. Synthesis of high quality two-dimensional materials via chemical vapor deposition. Chemical Science 6 (12), 675–6716.
Zhang, B.o., Wang, L., Zhang, C., Wu, S., 2022. High-performance cellulose nanofiber-derived composite films for efficient thermal management of flexible electronic devices. Chemical Engineering Journal 439, 135675.